Polagons: Designing and Fabricating Polarized Light Mosaics with User-Defined Color-Changing Behaviors

Ticha Sethapakdi
MIT CSAIL
USA

Laura Huang
MIT CSAIL
USA

Vivian Chan
Brown University
USA

Lung-Pan Cheng
National Taiwan University
Taiwan

Fernando Dall'Agnol
UFSC
Brazil

Mackenzie Leake
MIT CSAIL
USA

Stefanie Mueller
MIT CSAIL
USA

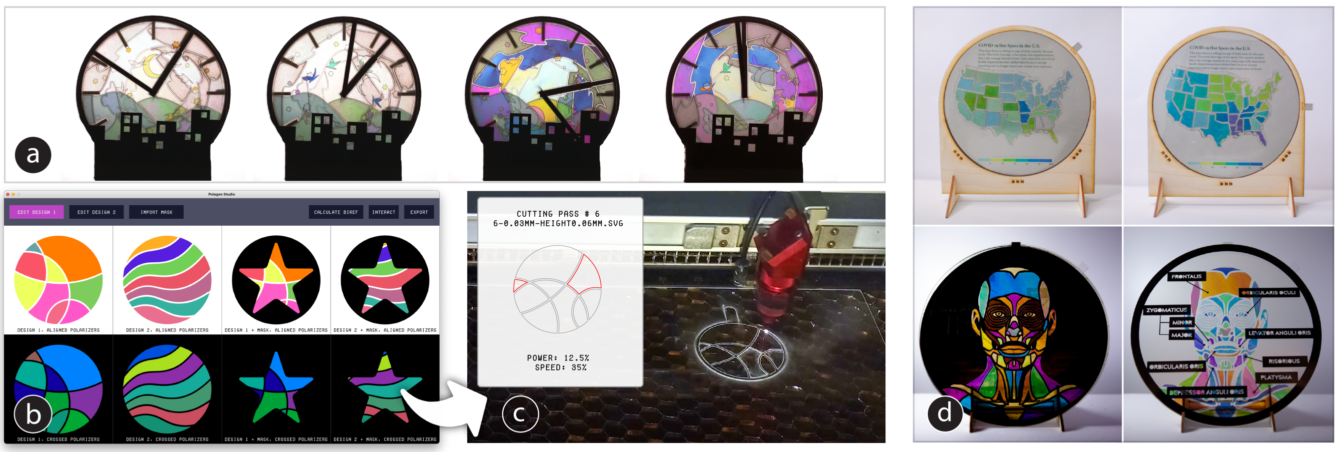

Figure 1: We introduce (a) *Polagons*: machine-made polarized light mosaics (PLMs) with user-defined color-changing behaviors. Our system comprises of (b) *Polagon Studio*, a tool for creating and visualizing Polagons, as well as (c) a custom fabrication process. We show how formalizing the process for making PLMs enables (d) new applications in a variety of contexts.

ABSTRACT

Polarized light mosaics (PLMs) are color-changing structures that alter their appearance based on the orientation of incident polarized light. While a few artists have developed techniques for crafting PLMs by hand, the underlying material properties are difficult to reason about; there exist no tools to bridge the high-level design objectives with the low-level physics knowledge needed to create PLMs. In this paper, we introduce the first system for creating *Polagons*: machine-made PLMs crafted from cellophane with user-defined color changing behaviors. Our system includes an interface for designing and visualizing Polagons as well as a fabrication process based on laser cutting and welding that requires minimal assembly by the user. We define the design space for Polagons and demonstrate how formalizing the process for creating PLMs can enable new applications in fields such as education, data visualization, and fashion.

CHI '23, April 23–28, 2023, Hamburg, Germany

ACM ISBN 978-1-4503-9421-5/23/04.
https://doi.org/10.1145/3544548.3580639

CCS CONCEPTS

• **Human-centered computing** → **Human computer interaction (HCI)**.

KEYWORDS

programmable materials, fabrication, optics, design tools

ACM Reference Format:
Ticha Sethapakdi, Laura Huang, Vivian Chan, Lung-Pan Cheng, Fernando Dall'Agnol, Mackenzie Leake, and Stefanie Mueller. 2023. Polagons: Designing and Fabricating Polarized Light Mosaics with User-Defined Color-Changing Behaviors. In *Proceedings of the 2023 CHI Conference on Human Factors in Computing Systems (CHI '23), April 23–28, 2023, Hamburg, Germany.* ACM, New York, NY, USA, 14 pages. https://doi.org/10.1145/3544548.3580639

1 INTRODUCTION

Conventional painting techniques rely on applying pigments, inks, and dyes to surfaces to create artistic imagery. But in the 1960s, some artists explored a new medium for painting: light. In particular, artists discovered materials with special properties that allowed them to change their appearance depending on how polarized light passes through them. This property is called *birefringence*. When a birefringent material is placed between two polarizing filters, the material is perceived as colored despite being naturally colorless.

Rotating the polarizer or birefringent material changes the incident angle of polarized light, which changes the emitted color.

A handful of artists have taken advantage of the unique properties of birefringent materials to make color-changing artwork [31], known as *polarized light mosaics* (PLMs). To create these mosaics, the artists use common birefringent household materials (e.g., cellophane films and packaging tape), cut out their desired shapes with scissors or craft knives, and control the color effects by carefully layering and rotating the cutouts [14]. While the majority of PLMs depict only a single image, some artists developed techniques for embedding multiple images into their mosaics. A notable example of this is the artist Austine Wood Comarow, who created elaborate morphing mosaics which she called "Polage" [27].

PLMs and birefringent materials have long sparked interest in artistic and scientific communities [10, 39]. However, this medium has not been widely explored and used — having a high barrier to entry due to a number of design and fabrication challenges. It takes time to acquire a deep understanding of how the material behaves, i.e., being able to precisely control the color effects requires an understanding of the underlying physics. Thus, users often resort to trial and error in crafting the desired colors and effects. Even a seasoned artist like Comarow, who developed this art form for over 40 years, iteratively built up the colors by repeatedly checking them with polarizers while layering cut sheets of cellophane [27]. While this approach can be helpful in some exploratory works, the lack of formal specifications and support tools for this medium hinders the creation of precisely specified designs.

Even with a comprehensive understanding of the underlying physics, the material is physically challenging to work with. As described above, the mosaics are made from cellophane or packaging tape, which are very thin and prone to warping or tearing. Cutting the material requires good motor skills and thus designs with complex geometries are difficult to make manually. The assembly process is yet another challenge: since color is affected by the incident angle of light, any subtle shift in the layers can produce undesired color results. Finally, complex mosaics may require hundreds of shapes [5], which are time-consuming to individually piece together by hand.

Encoding the underlying physics in a design tool that communicates the expected behaviors of the PLM can enable users to harness their unique properties for a wider range of applications. Thus, to address the aforementioned design and fabrication challenges, we present the first system that formalizes the process of making *Polagons*: PLMs with user-defined color-changing behaviors. Our system has two main components: *Polagon Studio*, a software toolkit for crafting PLMs, plus a fabrication process based on laser cutting and welding that requires simple manual assembly from the user. Polagon Studio automatically converts user-imported designs into PLMs and includes a visualizer that shows how different parameters, such as the image and polarizer orientations, change the design's appearance. When the user completes their design, Polagon Studio produces fabrication-ready files and generates instructions on how to use the laser cutter to fabricate the design. Our system enables makers to go beyond what was previously achievable manually, as it supports the creation of mosaics with both complex geometries and controlled color-changing behaviors. In summary, we contribute:

(1) An overview of the Polagon *design space*, including the constructions and supported color effects;
(2) A *software toolkit* that converts vector designs into Polagons and visualizes the color-changing behaviors;
(3) A *fabrication process* based on laser cutting and welding that requires minimal manual assembly;
(4) A *technical evaluation* of the color space for Polagons;
(5) Five *application scenarios* that demonstrate how Polagons can be used in practice;
(6) A set of *user designs* demonstrating our tool's expressive range.

2 RELATED WORK

Prior work in physical fabrication across many different domains has highlighted several challenges involving design and working with physically complex material properties. Our work draws inspiration from prior research on design tools, applications of optics and polarizers, and color-changing materials.

2.1 Digital design tools for physical crafts

Recently there has been much interest in the HCI community in designing tools that offer a wide range of interventions to support creativity, as outlined in Frich et al.'s recent survey [11], and physical fabrication with new a range of materials, as discussed in Bickel et al's recent survey [4]. Some tools, such as recent work on citrus fruit carving [25], focus support on digital design, while other tools, such as Rivers et al's tool for guiding sculpture through projection [36], put greater emphasis on the physical challenges of fabrication. Others, such as *SandCanvas* [20] for sand animation and a tool for computational handweaving [2], support design and execution in both the physical and digital worlds. Several tools have used digital design to create physical guides or jigs for creation, such as tools for wire-wrapped jewelry [45], wire sculpture [12], slab-based ceramics [16], and quilting [22]. Tools for domains, such as knitting [15, 28] and weaving [48], provide computational representations of craft processes through new programming languages and tools. Similar to the approach taken in many of these prior tools, Polagon Studio outlines the design goals and constraints of the domain of PLMs and then provides a suite of tools for addressing both the design and physical fabrication challenges. While many of these prior tools were developed through studying a popular creative domain, such as sewing, jewelry-making, and sculpting, Polagon Studio opens up new opportunities for creation in a domain with very few practitioners and little existing formal knowledge.

2.2 Color-changing materials

Helping users select colors for digital and physical creative applications has been explored for a wide variety of applications. For example, *Playful Palette* [40] explored how to help users select color palettes for digital painting. In physical applications many researchers have explored how to create tangible displays from color-changing materials. For instance, photochromic materials, which change color when exposed to light, can be used to create objects with re-programmable multicolor textures [17, 47]. Thermochromic inks, which change color with temperature, have also been used to create interfaces on a range of objects and surfaces, such as paper [33, 44], textiles [34, 41, 42], and even the body [18].

Whereas the above examples rely on specially-designed smart materials to create tangible displays, Polagons utilizes the inherent properties of cellophane to control the appearance of an object. Unlike typical smart materials, cellophane is a common household item, which gives users access to color-changing effects from materials that are easier to obtain.

2.3 Optics and polarizers

People have long been fascinated with leveraging reflective materials and creating optical effects. For example, researchers have used optical illusions to create volumetric displays [3, 26] and material displays [29, 50]. Recently several tools have been developed to help users reason about and control these physical properties for a range of applications. *Illumination Aesthetics* [46] is one such tool that helps users design and fabricate objects that shape and redirect light. Optics have also been used for touch input and interaction. For example, *PAPILLON* [6] used printed optics to enable bi-directional touch sensing on curved surfaces. While the aforementioned examples combine optics with electronics, researchers have also shown how optical effects can be used to passively display dynamic content. *WonderLens* [23] demonstrates how spatial operations on different lens types can provide dynamic visual feedback on paper, while *Lenticular Objects* [51] uses lenticular lenses to fabricate 3D objects with viewpoint-dependent textures.

Polarizers have seen a variety of real-world use cases. For instance, photographers have captured birefringent materials under polarized light to create unique pictures, while scientists have used polarized light imaging to see stress regions and molecular alignment in a wide range of applications [32]. Similarly, while polarizers have also been applied in a number of ways in HCI research, such as in AR/VR [19, 37, 49] and sensing [38], our focus is on display-based applications of polarizers. *Janus Screen* [21] uses polarizers to enable users to view content from both sides of a screen with a single projector. Most similar to our work is *PolarTag* [43], which shows how to create passive and unobtrusive tags using layers of birefringent material applied on top of a polarizing film. However, their examples solely use grid-like patterns that are created manually and do not provide a fabrication process for creating imagery with controlled color effects. Thus, to the best of our knowledge, there is no existing system that facilitates making PLMs.

3 WORKING PRINCIPLE

This section describes the working principle behind PLMs.

3.1 Materials

Most everyday materials are *optically isotropic*, meaning that the speed of light is constant for every angle that it passes through the material. Birefringent materials exhibit a unique property called *optical anisotropy*, wherein the speed of light varies depending on the angle of propagation through the material. Cellophane is a popular birefringent material among PLM artists because it is both inexpensive and easy to obtain (e.g., it is a common gift wrapping material). It is made from dissolving cellulose and then extruding the solution through a slit into an acid bath [30]. The *strain* refers to the amount of stretching or deformation that cellophane undergoes during this process, while the *strain direction* corresponds to the orientation of the forces applied to the cellophane. The amount of strain applied to the cellophane affects properties such as its thickness and birefringence, which influence the colors that can be produced. Variations in the manufacturing process change the material properties of the cellophane and artists leverage these variations to produce colorfully diverse PLMs. In a similar vein, we prioritized getting cellophane sheets of different thicknesses and birefringences to facilitate producing a wider range of colors.

3.2 Optics

Similar to how stained glass mosaics are made from disjoint shards of glass held together by plaster, PLMs are constructed from disjoint stacks of cellophane held together by an acrylic base. The assembled mosaic is then sandwiched between two polarizers (Fig. 2). For clarity, we refer to the polarizer that the viewer looks through as the *analyzer* and the second polarizer as the *polarizer*. When we say "the polarizers", we are referring to both the polarizer and analyzer.

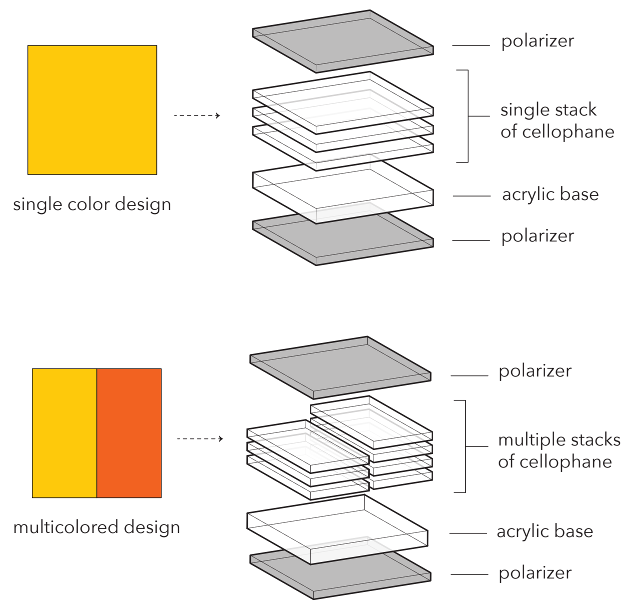

Figure 2: PLMs are made from stacking one or more pieces of clear cellophane together and sandwiching them between two polarizers. One can create multicolored designs by arranging stacks of different thicknesses.

The emitted color of a cellophane stack depends on four factors: the *thickness* of the stack (z in nm), the *birefringence* of the cellophane (β), the *angle of the analyzer* with respect to the cellophane strain direction (θ), and the *angle of the polarizer* with respect to the strain direction (ϕ). Using these factors, we can determine which color is shown when white light passes through the stack by applying the theory and equations described by Dall'Agnol et. al. [9].

Computing transmittance. To determine the color of a cellophane stack with thickness z and birefringence β when the analyzer and polarizer are at angles θ and ϕ, we first need to compute the *transmittance*, T_r, of the material at each wavelength λ of the white light that passes through the stack:

$$T_r(\lambda) = \sin^2\theta\sin^2\phi + \cos^2\theta\cos^2\phi + \frac{1}{2}\sin 2\theta\sin 2\phi\cos\left(\frac{2\pi\beta z}{\lambda}\right)$$

Note that T_r remains unchanged if θ and ϕ are reversed, which is the reason why the Polagon looks the same when it is flipped upside down. Since T_r depends on both β and z, this equation additionally implies that two stacks of the same thickness can still have different colors if their birefringence values are different.

Computing tristimulus values. After computing the transmittance T_r for each wavelength of white light, we can use the transmittance values to compute the tristimulus color values (X, Y, Z) across all visible wavelengths:

$$X = \int_{380}^{780} \bar{x}(\lambda) T_r(\lambda) \cdot E0 \, d\lambda$$
$$Y = \int_{380}^{780} \bar{y}(\lambda) T_r(\lambda) \cdot E0 \, d\lambda$$
$$Z = \int_{380}^{780} \bar{z}(\lambda) T_r(\lambda) \cdot E0 \, d\lambda$$

where $\bar{x}, \bar{y}$, and $\bar{z}$ are constants for each wavelength obtained from the CIE 1931 color matching functions with a 1nm stepsize [1], which describe how a standard human observer perceives colors. $E0$ is a constant radiance for all wavelengths, which is chosen as $1 \; W/m^2$. The limits of the integrals represent the visible light spectrum in nanometers.

Transforming Tristimulus Values into RGB. Finally, to determine the emitted color in RGB space, we apply a standard color space transformation to the tristimulus values:

$$[R, G, B]^\intercal = M^{-1} \cdot [X, Y, Z]^\intercal$$

where M is a linear transformation matrix calculated from RGB reference primaries [24].

Accommodating multiple cellophane types. The above equations make the assumption that stacks are constructed from a single type of cellophane. Mixing multiple types of cellophane, each with their own native thicknesses and birefringence, gives us access to a larger color palette. To capture these cases, we modify our original expression for T_r. Let β_i be the birefringence of cellophane film i and z_i be its thickness. Then:

$$T_r(\lambda) = \sin^2\theta \sin^2\phi + \cos^2\theta \cos^2\phi + \frac{1}{2}\sin 2\theta \sin 2\phi \cos\left(\frac{2\pi \sum_i \beta_i z_i}{\lambda}\right)$$

4 DESIGN SPACE

We use our knowledge of the material properties and physics principles to inform a design space for Polagons. Here we describe the mosaic constructions and achievable color effects in increasing order of complexity.

Single color mosaics and color-to-clear transitions. The most basic mosaic uses a single layer of cellophane sandwiched between the two polarizers, which results in a single-colored design. Different single-colored shapes can be created by cutting pieces from the cellophane and arranging them on the acrylic base with small gaps in-between. When both polarizers are aligned with the cellophane's strain direction, the mosaic appears transparent (Fig. 3a). As the mosaic is rotated, its appearance becomes progressively more colorful (Fig. 3b), reaching its maximum saturation when its orientation relative to the polarizers is 45° (Fig. 3c). Rotating it further fades the color until it becomes colorless again at 90°. Thus, the mosaic colors are identical at 90° angle differences, i.e., its appearance is the same at 45°, 135°, 225°, and 315°. Assuming that the relative angles are the same, flipping the mosaic upside down also does not change its colors.

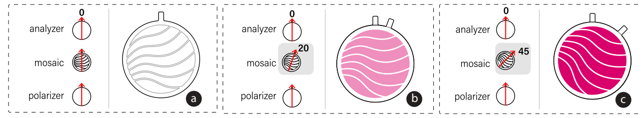

Figure 3: Changing the opacity of a mosaic by adjusting its orientation with respect to the polarizers.

Complementary colors. The alignment of the polarizers with respect to each other also affects the appearance of the design. Polarizers are parallel when they are 0° with respect to each other and orthogonal when they are 90° to each other. Colors under parallel (Fig. 4a) and orthogonal polarizers (Fig. 4b) are complementary to each other. Thus, by keeping the mosaic static and rotating either the analyzer or polarizer, we can achieve two different colors with a single layer of cellophane. Furthermore, parallel polarizers let light pass through, while orthogonal polarizers block light. Thus, areas not covered by cellophane are clear under parallel polarizers and black under orthogonal polarizers.

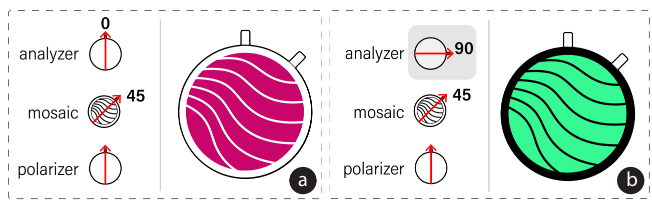

Figure 4: Inverting colors by orienting the polarizers orthogonally to each other.

Mixing colors and multicolored mosaics. We can "mix" colors by stacking multiple pieces of cellophane together and then create multicolored designs by arranging individual color stacks to form an image (Fig. 5a). Assuming that the strain direction is the same for each color stack, the aforementioned fading and inversion effects work in the same way as the single color variants (Fig. 5b).

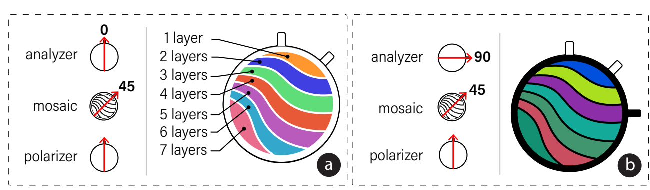

Figure 5: Multicolored mosaics are composed from stacks of cellophane of different heights.

Color-to-color transitions. We can create transitions between two mosaics by placing them on top of each other before sandwiching them between the polarizers (Fig. 6). Recall that mosaics are colorless at 0° rotations and reach full saturation at 45° rotations relative to the polarizers. By positioning the mosaics at a 45° offset to each other, we ensure that one mosaic is fully saturated only when the other is fully colorless. Rotating the mosaics in tandem results in a "crossfading" effect. The same effect can be achieved by keeping the mosaics static and instead rotating both polarizers.

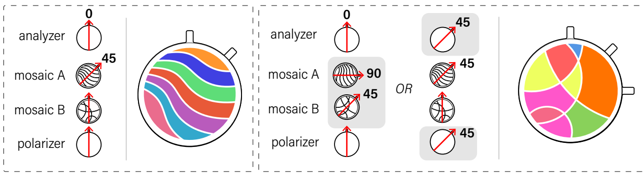

Figure 6: Performing color-to-color transitions by rotating either the mosaics or the polarizers in tandem.

Masking images. We can apply a "masking" effect to the mosaics by inserting a third polarizer between the topmost mosaic and analyzer (Fig. 7). The mask's visibility depends on its alignment relative to the analyzer. As polarizers block light when they are orthogonal, the mask is fully opaque when it is orthogonal to the analyzer (Fig. 7a,b) and transparent when the two are parallel (Fig. 7c,d).

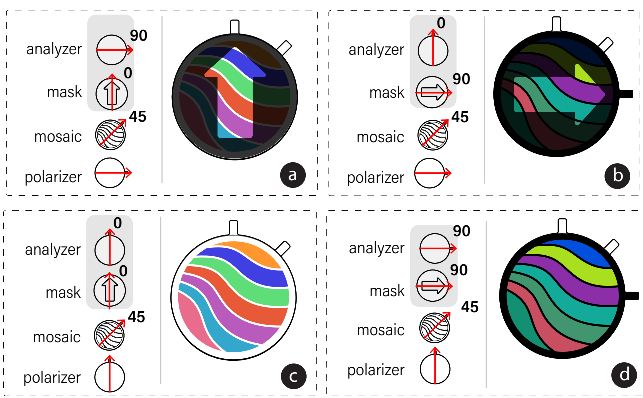

Figure 7: Changing the visibility of the arrow-shaped masking layer by adjusting its orientation relative to the analyzer.

Summary of mosaic constructions. Figure 8 summarizes the different mosaic constructions for Polagons. The *single mosaic* construction consists of only one mosaic sandwiched between two polarizers (Fig. 8a), which yields a single image that can transition from transparent to opaque, as well as invert its color. The more advanced *double mosaic* construction contains a second mosaic layer between the polarizers (Fig. 8b), which adds support for two images that can cross-fade into each other. The *single mosaic, single mask* and *double mosaic, single mask* constructions are variants of the first two constructions, which make use of a third polarizer to mask out parts of the mosaics (Fig. 8c,d).

The most complex designs crafted by artists make use of single mosaic constructions with or without a mask [8]. Dall'Agnol et al. [9] demonstrated a double mosaic construction using simple geometries and a small set of colors. Our system extends these methods by not only supporting double mosaic constructions with complex geometries and a wide color range, but also including double mosaic, single mask constructions which have not been built before by hand.

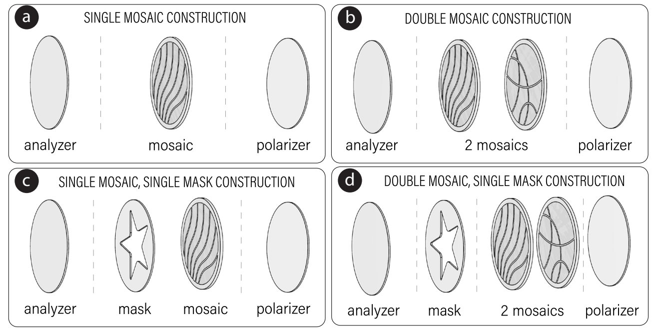

Figure 8: All Polagon constructions.

5 POLAGON STUDIO

Polagon Studio is a toolkit that lets users design Polagons based on the mosaic constructions described in Section 4. The core workflow consists of choosing a mosaic construction, creating keyframes and exploring the color space, interacting with the virtual PLM to preview the color transitions, and exporting the design for fabrication.

5.1 Choosing a Polagon construction

Upon startup, Polagon Studio shows users design templates based on the four core Polagon constructions. Hovering over a construction shows an animated preview of how that particular construction works in practice. The template that the user picks determines the complexity of their final design. Once users select a design template, Polagon Studio loads the template files into the main window (Fig. 9a). Users can then modify the existing template files or load custom designs into the interface.

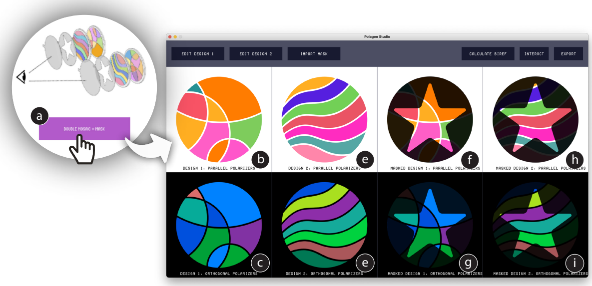

Figure 9: Selecting a design template (a) loads its corresponding template files into Polagon Studio. The main window is then updated to display (b-i) all the keyframes of the design, depending on the orientation of the constituent layers. While the keyframes are laid out in a grid in the interface, note that any keyframe can transition into any other keyframe in the fabricated design.

5.2 Creating keyframes

A *keyframe* represents a view of the Polagon in which either of its mosaic layers is at full opacity. The main window of Polagon Studio shows all the keyframes of a design. For example, for a double mosaic, single mask construction, this creates 8 keyframes: the first mosaic under parallel and orthogonal polarizers (Fig. 9b,c), the second mosaic under parallel and orthogonal polarizers, (Fig. 9d,e), and each of these 4 keyframes with a switchable transparent-to-opaque mask (Fig. 9f,g,h,i). In the fabricated PLM, the user can change any keyframe into any other keyframe by rotating the constituent components of the mosaic.

Preparing a mosaic design. Users can create their mosaic designs in a vector graphics editor (e.g., Adobe Illustrator). A valid mosaic is made from closed, colored shapes that are spaced at least 1mm apart. Having filled shapes ensures that Polagon Studio can parse the design, while the spacing between shapes prevents adjacent shapes from being stuck together during fabrication. Finally, the design cannot have shapes that are fully contained within each other. Once the user has finished their mosaic design, they can save it as an SVG file and import it into Polagon Studio.

Loading a mosaic into Polagon Studio. When the user imports their design, the interface remaps the colors in the design to their closest matching colors under aligned polarizers and loads the "Edit Design" window (Fig. 10).

Exploring the color space. The "Edit Design" window allows users to explore the available color palette and make changes to the colors in their mosaic. Polagon Studio comes equipped with a pre-populated database of the feasible color palettes and their stack compositions, based on our supply of cellophane (0.023mm, 0.03mm, 0.035mm, 0.045mm, 0.053mm). We provide two color palettes: one that stores all possible colors under parallel polarizers (which we refer to as the 'white background' palette since parallel polarizers allow light to pass through) and another that stores all possible colors under orthogonal polarizers (which we call the 'black background' palette since orthogonal polarizers block light and give users access to black).

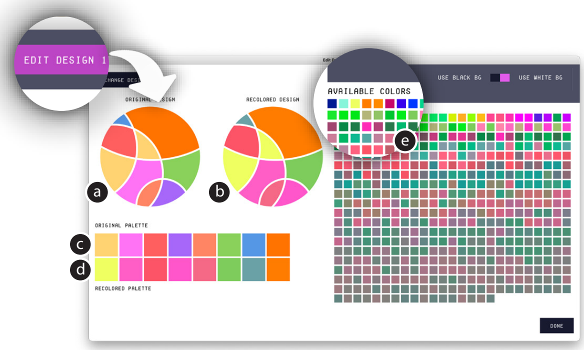

Figure 10: The 'Edit Design' window, which loads when the user imports a mosaic. The window shows (a) the original design, (b) the recolored design, (c) their original color palette, (d) the recolored palette, and (e) the available color palette.

Within the "Edit Design" window, the user can take several actions:

(1) *Use different backgrounds.* While designs are recolored with the white background palette by default, users may opt to recolor their design using the black background palette (Fig. 11). This later causes them to see the original colors in their design when the polarizers are orthogonal and the inverted colors when the polarizers are parallel.

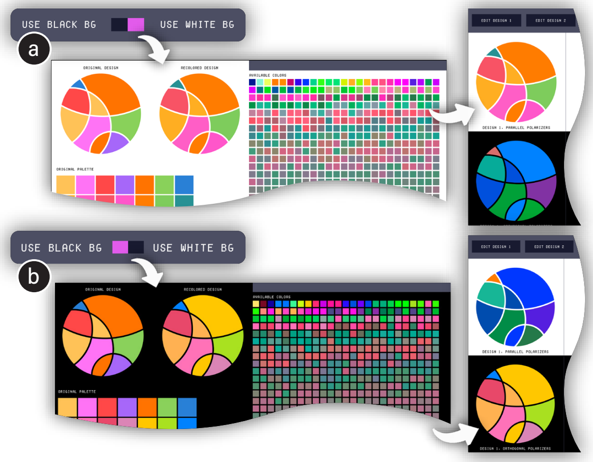

Figure 11: Users can recolor their design based on the (a) "white background palette", which shows the original colors under aligned polarizers, or the (b) "black background palette", which shows the original colors under crossed polarizers. Users can also see which colors are available under each polarization condition.

(2) *View material requirements.* Hovering over a swatch in the available color palette displays a tooltip that shows the quantity and types of cellophane that the color is made from (Fig. 12).

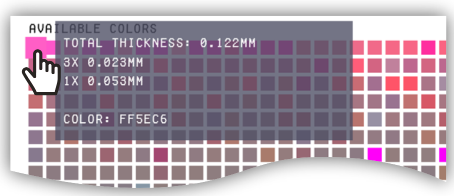

Figure 12: Users can view the cellophane composition for a swatch by hovering over it.

(3) *Filter cellophane types.* Users can refine the color palette by filtering cellophane types, which can be useful if the user only has certain thicknesses of cellophane available. Filtering the palette automatically recolors the design to use the closest matching colors in the remaining color palette.
(4) *Adjust design colors.* To change a color assignment, users first select the corresponding swatch from the color palette of their design. This rearranges the overall color palette to display the most visually similar swatches first. The user can then select a swatch from the overall color palette to replace the color in their design.
(5) *Save assignments.* The user selects 'done' to confirm the color assignments. This updates the main window to show the first mosaic under both parallel and orthogonal polarizers.

Adding a second mosaic. After the first mosaic is imported, users can choose to add a second mosaic by selecting "Edit Design 2". The workflow for importing and editing the second mosaic is identical to that of the first.

Preparing and importing the mask. Users similarly create the mask using a vector graphics editor and save it as an SVG that can be imported into Polagon Studio. A typical mask is made from a single connected shape that is the size of the mosaic. Polagon Studio renders the mask with a semi-transparent black fill color, regardless of how it was colored in the original file.

5.3 Interacting with the virtual Polagon

Users can interact with the virtual Polagon and visualize the different color changing behaviors via the "Interact" window (Fig. 13). The left side of the "Interact" window shows the Polagon decomposed into its constituent components (i.e., analyzer, mask, mosaics, and polarizer), as well as the orientations of each. The right side shows the effect that those rotations have on the Polagon's appearance. The user can adjust the orientation of each component by either rotating its corresponding knob or entering a rotation value. Users can also rotate multiple components at once by clicking and dragging the knobs while pressing a hot key.

Figure 13: The "Interact" window shows the effects of rotating the constituent parts of the Polagon.

Previewing the Polagon on a 3D model. To allow users to see how their Polagon looks in context with their physical object, we created a plugin for a 3D CAD tool (*Rhinoceros*), that interfaces with Polagon Studio. When the user selects "create snapshot" from the "Interact" window, the system generates a 2D texture file from the Polagon's current appearance. The 3D plugin then automatically loads this texture file and previews it with the model (Fig. 14a). Selecting "create snapshot" again refreshes the texture file and updates the model accordingly (Fig. 14b). The displayed texture additionally includes arrows corresponding to the orientations for the polarizer and analyzer, which can help users to better plan the rotation mechanisms for their physical object.

5.4 Adding new cellophane types

By default, our user interface is populated with the color palette derived from the cellophane types we had access to. If users had to buy cellophane with different native thicknesses or from different manufacturers, Polagon Studio provides a way for users to update the database to reflect their supply of cellophane (Fig. 15).

Measuring thickness and birefringence. Users can typically obtain thickness information from their manufacturer. After they

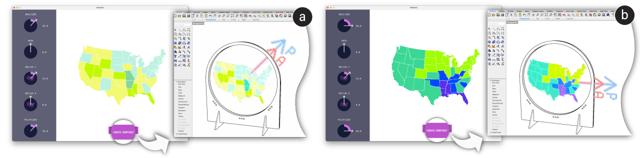

Figure 14: Users can save the mosaic's current appearance as a texture and (a) preview it on a 3D model. As the user interacts with the mosaic, they can refresh the window to see (b) the changes reflected on their model.

enter the thickness, the user interface shows a preliminary color palette under parallel polarizers. However, those colors are computed based on a default birefringence and need to be further adjusted based on the birefringence of the user's cellophane. As manufacturers do not typically disclose birefringence information, determining the birefringence of cellophane is nontrivial; although scientists use polariscopes to accurately measure the birefringence of cellophane, most users do not have access to such specialized equipment. Thus we provide a software-based approach for estimating the birefringence. First, the user has to cut out individual pieces of their cellophane and stack them (while keeping the orientation consistent) to form a basic color palette (Fig. 15a). They can then check their physical palette against the preliminary palette in the interface (Fig. 15b). If the estimated colors do not match well, the user can adjust the birefringence value until the estimated colors are as visually close to the physical colors as possible (Fig. 15c).

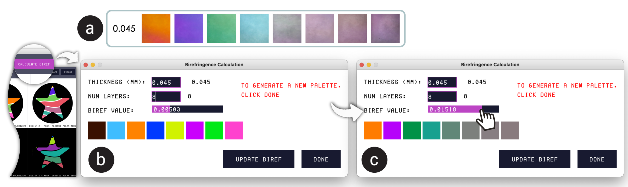

Figure 15: To add a new cellophane type to the database, users (a) construct a physical color palette, (b) enter the material thickness and check the palette against a preliminary palette in the interface (based on a default birefringence value), and (c) update the birefringence estimation until the predicted colors match the physical colors.

Generating the new palette. Once the user confirms the new birefringence value, the system re-computes the feasible color palette under parallel and orthogonal polarizers by combining the new type of cellophane with the existing types in the database.

5.5 Preparing the design for fabrication

Once the user is ready to fabricate their design, they can export fabrication-ready files (Fig. 16). Each fabrication file corresponds to a single cutting pass, or "fabrication step". The files corresponding to the mosaic layers are automatically exported at a 45° offset to each other, which ensures that only one mosaic is visible at a time.

6 FABRICATION

Since the color effects rely on the cellophane layers being properly aligned, users have to ensure that the strain direction is consistent

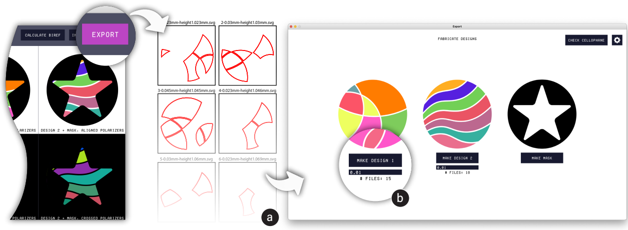

Figure 16: Exporting a Polagon for fabrication generates (a) fabrication-ready files. Polagon Studio generates multiple cutting files for (b) each mosaic layer and a single file for the mask layer.

across all sheets prior to fabrication. When users select 'check cellophane' in Polagon Studio's export window, they are shown a visual reference for what the colors should look like when all sheets are overlapping (Fig. 17). Users can then overlay their cellophane sheets in a similar fashion and verify that they are all aligned with respect to each other by comparing the colors under aligned polarizers with the digital reference. To correct the alignment, users rotate the cellophane sheet(s) until the colors match.

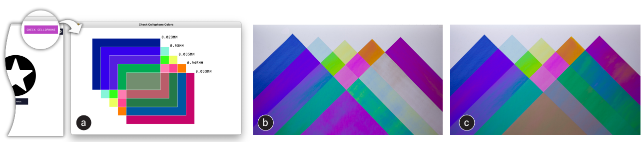

Figure 17: Calibrating the strain direction by overlaying one layer of each cellophane thickness on top of each other and comparing the colors to (a) the reference in the interface. (b) Incorrectly aligned sheets will have regions that are visibly dissimilar to the reference while (c) correctly aligned sheets will match the reference.

To make a Polagon, users follow the fabrication instructions from the interface (Fig. 18a,b). The process of fabricating a mosaic involves placing a cellophane sheet into the laser cutter (Fig. 18c), running the cutting process (Fig. 18d), removing the outer area of the cellophane sheet (Fig. 18e), and repeating until all fabrication steps are complete (Fig. 18f). For double-mosaic constructions, users assemble the final Polagon by stacking the two mosaics on top of each other. Since the first mosaic was cut at a 45° angle, the correct assembly requires the user to rotate it to its original orientation before stacking the second mosaic on top. Users can then place the mask layer on top of the mosaics in the same orientation as their original design. They complete the Polagon by sandwiching the layers between two polarizers.

7 APPLICATION EXAMPLES

We present five application examples to illustrate how each Polagon construction can be used in practice. To demonstrate how our system can be used in different settings, Author 3 designed and fabricated applications 7.1 to 7.3 in Taiwan using a 150W Trotec Speedy 300 laser cutter, while Author 1 designed and fabricated applications 7.4 and 7.5 in the United States using a 100W ULS PLS 6.150D laser cutter.

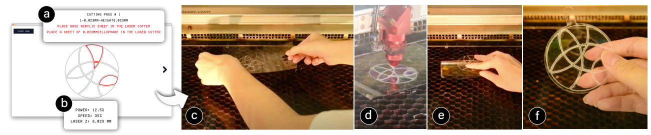

Figure 18: At the start of each fabrication step, Polagon Studio displays (a) which cellophane type they must load into the laser cutter and (b) what laser cutting settings to use. Each fabrication step involves (c) placing a cellophane sheet into the laser cutter, (d) running the cutting process, (e) removing the excess cellophane, and repeating until (f) all steps are complete.

7.1 Passive display

We incorporated a Polagon into a sliding glass door to create a passive display that reminds users to close the door when it is open (Fig. 19). To do this, we affixed a single mosaic and polarizer to a glass panel and attached the analyzer to a sliding glass door, which causes the display to be visible when the door slides open and overlaps with the panel.

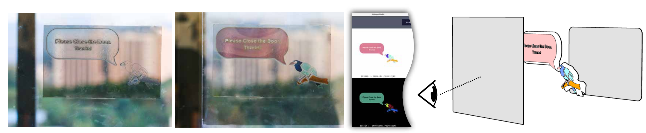

Figure 19: A glass door display made with a single mosaic.

7.2 Reconfigurable fashion components

To show how Polagons can facilitate rapid personalization, we created a pair of reconfigurable glasses inspired by the "kaleidoscopic glasses" worn at festivals (Fig. 20). Each lens consists of a double mosaic layer with a single mask and integrated polarizers. Since each lens produces 8 keyframes, there are 64 unique configurations in total. To allow users to quickly access the different keyframes of the design, we used the orientation guides to add notches to the border of the frame as reference points for the rotations.

Figure 20: A pair of reconfigurable glasses. Each side was made with two mosaics and one mask.

7.3 Mechanical animations

We combined Polagons with the rotational mechanisms in a clock to create a color-changing clock face (Fig. 21). This design combines two double-mosaic constructions, which was possible by exporting from Polagon Studio twice. The layers containing the birds and night sky are attached to the minute hand and offset by 45°, which allows them to fade in and out of each other. The clouds rotate with the hour hand while the mountain background is a static element attached to the back of the clock. Finally, the cityscape is a static masking layer that is always visible.

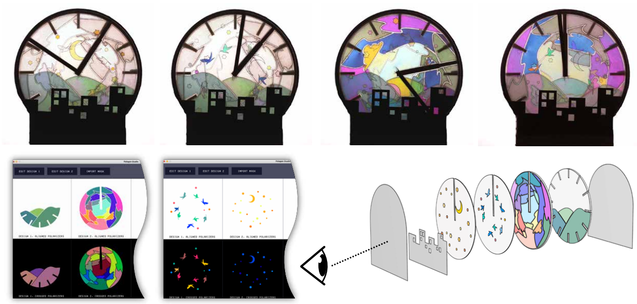

Figure 21: An animated clock made with two double mosaics and one mask.

7.4 Disclosing user-dependent information

To explore how we can use Polagons to show user-dependent information, we created an anatomy diagram that uses a single mosaic, single mask construction with one polarizer and two analyzers (Fig. 22). The two analyzers are orthogonal to each other and are held by two users. If both users were to look at the diagram from the same point of view, one will see the diagram without the labels while the other will see it with the labels.

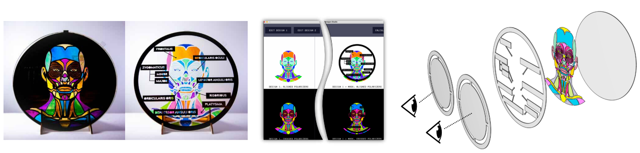

Figure 22: An anatomy diagram with user-dependent views, made with one mosaic, one mask, and two analyzers.

7.5 Data physicalization

We used a double mosaic construction to create a data physicalization (Fig. 23) that shows how the COVID-19 hot spots in the United States changed between July and August 2021 [7]. The viewer switches between the July 2021 and August 2021 charts by rotating the polarizers in tandem. We modeled the map frame in a 3D CAD tool and used the orientation guides from Polagon Studio (Fig. 14) to determine where to engrave the date labels. Finally, we printed the title and chart legend on transparency film and placed it behind the Polagon, giving us control over which elements of the design remain visually unchanged by polarizer rotations.

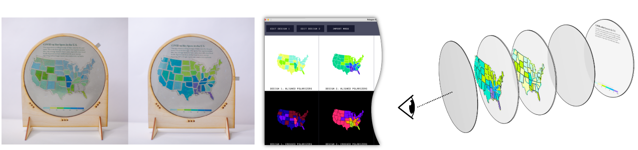

Figure 23: An interactive map made with two mosaics.

8 IMPLEMENTATION

The Polagon Studio interface was created with Processing. We additionally run a Python Flask server in the background, which passes data to and from Processing, performs the color calculations, and generates the required output.

Storing colors in the database. After computing the feasible color palette (Section 9.1), we store each color along with its stack composition in the database. In some cases, there may be multiple compositions that map to the same color. Since we store a single representation in the database, we prioritize the stack composition that requires the fewest number of layers of cellophane. In case of ties, we pick the composition that uses fewer types of cellophane.

Recoloring mosaics. When a mosaic is loaded into the user interface, we iterate through each shape in its SVG file and compute the color distance [35] between its fill color and each swatch in the feasible palette. The mapped swatch in the palette is the one that minimizes the distance.

Updating the appearance. To determine the appearance of the Polagon when its constituent layers are rotated in the "Interact" window, we applied the equations described in Section 3.

Mosaic appearance. As before, we let θ be the rotation of the analyzer relative to the mosaic and ϕ be the rotation of the polarizer relative to the mosaic. Let $\sum_c \beta_c z_c$ represent the composition of some color c. Then for each original color in the design, it is recolored according to the calculations in Section 3 using values θ, ϕ, and $\sum_c \beta_c z_c$. We then compute α, the opacity of the mosaic. Let $\theta' = |\theta \pmod{90°}|$. Then:

$$\alpha = \begin{cases} \texttt{map}(\theta', 0, 45, 0\%, 100\%) & \text{if } \theta' \leq 45° \\ \texttt{map}(\theta', 45, 90, 100\%, 0\%) & \text{if } \theta' > 45° \end{cases},$$

where $\texttt{map}(x, s_1, t_1, s_2, t_2) = s_2 + \frac{(x-s_1)(t_2-s_2)}{t_1-s_1}$.

Mask appearance. Since the mask is always rendered in black, the only value that changes is its opacity. If Θ is the angle of the mask relative to the analyzer, the opacity of the mask is $\texttt{map}(\Theta, 0, 90, 0\%, 100\%)$.

Preparing designs for fabrication. Our system splits the fabrication process into several fabrication steps. Initially, each shape is made of zero layers of cellophane. Each fabrication step adds one layer of cellophane to the shapes in the design that require additional layers to create their color. At each step, each shape has a *current height*, which is the total thickness of the layers of cellophane that currently make up that shape. To ensure that the next layer of cuts adheres well, our system guarantees that:

(1) The set of shapes to be cut all have current heights that differ by at most ε from each other;
(2) All shapes that are about to be cut have height at most ε shorter than the current tallest shape

Together, these properties ensure that the cellophane can lie flat on the next set of shapes to be cut. To achieve this, the system iterates through each type of cellophane and considers the sets of shapes that require at least one layer of that cellophane, at least two layers, at least three, and so on. For each such set of shapes, the shapes are ordered by their current height, assuming that all previously considered cellophane types and layers have been cut. The shapes in the set are then greedily partitioned into groups of height differing by at most ε (for our examples, we typically set $\varepsilon = 0.1$). Each group is saved as a fabrication step. Finally, the fabrication steps are sorted by the height of the shortest shape in each step. This ensures that all shapes have the stack composition corresponding to their color and that the heights of the shapes in each fabrication step satisfy Properties (1) and (2) above.

Since we keep power and speed constant for all types of cellophane, we use the number of cutting passes to cater to different thicknesses. Thus for each fabrication file, we set the number of copies of each shape to the number of cutting passes required for that file's cellophane type. Finally, we format all shapes to use vector cut settings (e.g., a red stroke with a width of 0.0001px).

9 TECHNICAL EVALUATION

We compute the theoretical color gamut given our cellophane types and compare the physical colors to their predicted values.

9.1 Determining color gamut

To determine the color gamut for our supply of cellophane, we calculated all possible colors from stacking different cellophane types. We only considered a total stack thickness of at most $z = 0.25$mm, as we found that thicknesses larger than that produced mostly gray and indistinguishable colors. For all possible values of $\sum_i \beta_i z_i$, such that $\sum_i z_i \leq 0.25$mm, we used the procedure described in Section 3 to determine the most saturated colors under parallel and orthogonal polarizers, i.e., the values at $\theta = \phi = 45°$ for parallel polarizers and $\theta = 45°$, $\phi = -45°$ for orthogonal polarizers. Based on this procedure, we found that our stock of cellophane produces 492 unique RGB values for each orientation. We then plotted these values on the CIE-xy color gamut chart (Fig. 24). For colors predicted outside the gamut, we follow the procedure from Dall'Agnol et al. [9] and project them onto the edge of the gamut region, as those colors cannot be represented in a monitor display. From this chart, we see that points are distributed along the perimeter of the RGB triangle, which demonstrates that our palette captures the spectral colors. Our gamut also reveals several clusters of points in the green and purple regions, which indicates that our cellophane is biased towards producing green and purple hues. In addition, our gamut has a large cluster of points in the center, which suggests that our palette includes many desaturated colors that may be hard to distinguish. Note that these insights are based on the cellophane we selected; a different set of materials would yield a palette with a different quantities and distributions of colors.

9.2 Checking color fidelity

To verify that our model makes reasonable predictions, we compared colors predicted by our system to their physical counterparts. For each cellophane type, we created small (34mm×34mm) color chips from a single layer of material. We then digitally generated 100 random cellophane compositions from our available cellophane types and physically reconstructed them by aligning and stacking the color chips. We photographed the reconstructions under a single white light source.

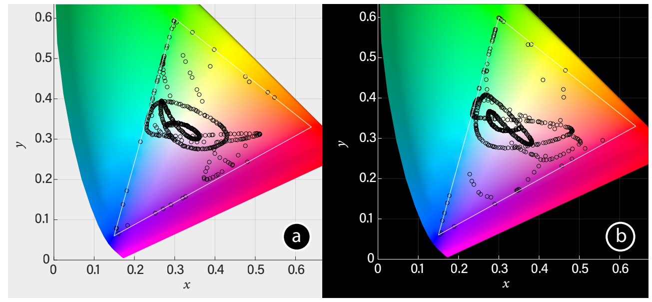

Figure 24: Color gamut given our supply of cellophane under (a) parallel and (b) orthogonal polarizers.

Quantifying differences between colors remains an open challenge and there is no universal metric that fully captures the nuances of human vision [13]. For our experiments, we picked a weighted Euclidean distance function [35] to compute the RGB distance between the predicted and physical swatch pairs. We chose this metric because it is a stable algorithm that performs comparably to perceptually uniform color models. Figure 25 visualizes the results for the 5 most similar and least similar swatches from our experiment. On a scale of 0 to 765 (i.e., 0 to 255 per RGB channel), the mean color distance across all pairs is 119.01 (σ : 42.93), which yields an accuracy of 84.44%. These results confirm that our modified transmittance equation, which accounts for different cellophane thicknesses and birefringence values, yields predictions that approximate the physical colors well. In practice, we also found that users do not see these visual differences as being more significant than that of standard fabrication processes which involve translating a digital color into its physical representation (e.g., colored 2D or 3D printing). We discuss this in more detail in Section 11.

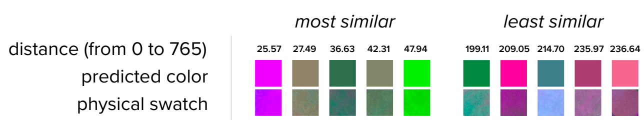

Figure 25: A comparison of the predicted and physical results for the 5 most similar and least similar swatches from our experiment.

10 USER DESIGNS

To get a better understanding of our tool's expressive range, we invited designers to use Polagon Studio to develop new applications for PLMs.

10.1 Participants

We recruited 6 participants (4 female; mean age 23.8) via convenience sampling. Participants were selected based on self-reported expertise in vector and/or CAD drawing programs. All participants had limited to no prior knowledge of PLMs and none have created them in the past. Participants came from a range of vocational backgrounds: three from architecture, two from computer science, and one from mechanical engineering.

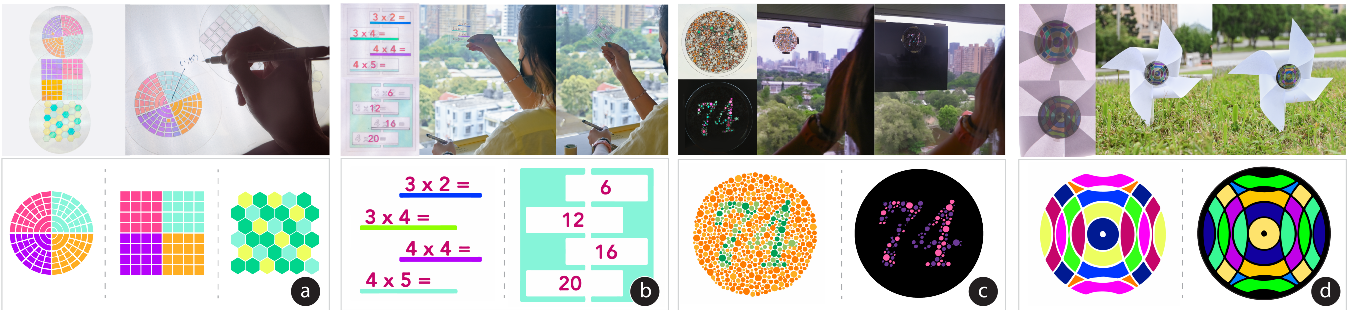

Figure 26: User-created designs: (a) an interactive whiteboard, (b) animated arithmetic, (c) an Ishihara test, and (d) a wind-powered bird deterrent.

10.2 Data collection

Prior to the activity, participants filled out a questionnaire asking them to provide their academic background, level of proficiency in using vector and/or CAD drawing programs, level of familiarity with color-changing materials, and demographic information. We then met with each participant in-person and took notes during the sessions. At the end of the design process, we had participants complete an exit survey that asked for additional qualitative feedback on the effectiveness of the UI and scope of applications.

10.3 Procedure

Before meeting the participants, we provided them with a video introducing our system and example applications. We then asked them to brainstorm 5-10 possible applications for PLMs. In a followup meeting, we explained how PLMs are made and demonstrated how to use our tool. We then let participants use the interface to interact with the design templates and familiarize themselves with the color-changing effects. During this exploration phase, we asked participants to describe how each component affects the appearance of the mosaic. We validated their understanding by asking them to complete a sample task (e.g., "make the background black and keep the striped texture visible").

Once participants familiarized themselves with the color-changing behaviors, we discussed their application examples in more detail and asked them to select one idea to refine and prototype in Adobe Illustrator. Participants then imported their vector designs into Polagon Studio, adjusted the colors as needed, and interacted with the virtual mosaic. Once participants were satisfied with the interactions, they exported the fabrication files from Polagon Studio. The authors then fabricated a subset of the participants' designs separately and had a followup meeting with each of those participants to discuss whether the outputs aligned with their expectations.

10.4 Results and participant feedback

Below, we describe the participants' designs, discuss the affordances of our tool, and summarize the lessons learned.

Polagons can be used for a variety of application examples. Altogether, participants created a diverse set of application examples that spanned the full design space for Polagons. Figure 26 shows an example gallery of P1 through P4's applications. We did not fabricate P5 and P6's applications as they were conceptually similar to examples presented in Section 7.

Interactive whiteboard (3 single mosaics). P1 used 3 single mosaics to make hideable reference guides for a transparent whiteboard (Fig. 26a). P1 created components comprising of radial, square, and hexagonal grids, which users can rotate to fade in and out of view.

Animated arithmetic for children (double mosaic). To make math more engaging for children, P2 used a double mosaic construction to create arithmetic equations wherein the left hand expressions fade to reveal the answer (Fig. 26b). Users rotate the polarizer and analyzer in tandem to change the visibility of the expression.

Ishihara test (single mosaic, single mask). P3 designed an Ishihara test that explores how to measure color-blindness on a continuous scale using a single mosaic, single mask construction (Fig. 26c). As the user rotates the analyzer, the test gradually reveals the number.

Wind-powered bird deterrent (single mosaic). P4 designed a pinwheel that is meant to scare wild birds away from potentially dangerous structures (Fig. 26d). The pinwheel is attached to the polarizer, which causes the mosaic to flash when the wind blows.

Morphing data visualization (double mosaic). To allow users to view data in two different ways, P5 used a double mosaic construction to design a pie chart that transitions into a bar graph. The transition occurs when the user rotates the polarizers in tandem.

Color-changing tree (double mosaic, single mask). P6 created an artistic design that depicts a tree that changes with the seasons. Rotating the mosaic layers causes the tree to alternate between its spring (tree with leaves) and fall (tree with apples) views. Rotating the analyzer reveals the winter view, which uses a mask to obscure everything except for the tree trunk and branches.

Polagon Studio supported different design approaches. Since Polagon Studio uses the standard SVG format for mosaics, participants had the flexibility to use different workflows when creating their designs. While some participants drew their designs from scratch (P1, P2, P4), others were able to repurpose existing designs from other sources (P3, P5, P6). For example, both P3 and P6 found images of their desired designs online and used Illustrator to automatically vectorize them. They then made only minor adjustments to the design to ensure that it is a valid mosaic. P5 downloaded two charts from the vega-lite example gallery, and similarly made only minor modifications. In all cases, participants were able to import their desired designs into Polagon Studio and quickly prototype the color-changing behaviors.

Participants built intuition for how PLMs work. All participants appreciated the ability to visualize designs before constructing the mosaic, noting that the "Interact" window helped them "build intuition about what effect each layer has on the image" (P5) and "understand some of the science behind the effects" (P2). When asked to change the mosaic to take on a specific appearance, all participants were able to quickly rotate the appropriate components of the mosaic to achieve the desired result. P4 noted that being able to interact with the template designs was "a perfect starting point for completely novice users". P6 similarly commented that "having examples and playing with the interface helped [them] understand the system well enough to design something". Furthermore, all participants were able to appropriately scope their applications, with minimal guidance, to fit the constraints of the mosaic constructions.

Participants who had their designs fabricated felt like the outputs met their expectations. When asked to rate on a scale of 1-5 (1 being not at all to 5 exactly) how much the output looked like what they expected from their original design, all participants answered 4 or 5. P2, who gave a score of 4, explained that their score was due to slight differences in color and the material was less transparent than they expected. P1 and P4, who gave scores of 5, noted that they prioritized global color contrast over local color accuracy—so any discrepancies did not affect the overall look and feel of the mosaics. P1 and P2 felt that the differences between the digital and physical representations of Polagons are no greater than that of standard fabrication processes, such as 2D and 3D printing. P1 added that while users would have to be cognizant of these differences when designing with Polagon Studio, it does not make the tool less valuable to the "prototyping" process.

11 DISCUSSION AND LIMITATIONS

Here we discuss limitations and future opportunities for Polagons.

11.1 Prototyping vs. simulation

We found that Polagon Studio works best as a medium fidelity prototyping tool. User feedback indicates that the suite of features offered by Polagon Studio can help users understand the design constraints for mosaic construction, translate a design into a valid mosaic, and get a sense of what the outputs will look like. At the same time, the visualizer cannot completely replace the experience of interacting with physical mosaics as it does not fully simulate PLM behaviors. While the underlying model is based on estimated birefringence values and assumes that the mosaic is viewed under white light, the physical colors may differ slightly from the predictions. The visualizer also does not account for the texture of the cellophane, how colors look under different lighting conditions, or how colors might change when the mosaic is viewed from different angles. With the current mathematical model, the system only scratches the surface of what is possible with PLMs. Some participants were interested in seeing the effects of rotating the mosaics separately (P1, P5, P6) or were curious to see more complex mosaic occlusions (P5), which are not currently supported by the tool. With a more sophisticated model, designers can potentially discover new use cases and explore the full spectrum of PLM interactions.

11.2 Supporting novice practitioners

The high level abstractions provided by Polagon Studio enabled novices to PLMs to build intuition on how they work. While our system serves as a "black box" for making PLMs, we found that providing more transparency by including lower-level concepts may help users improve their understanding of the material. Participants suggested including more information in the interface (P2, P5, P6) to better aid novices in understanding PLMs. P1 felt like it could be useful to lock turns at common angles of interest. P5 and P6 suggested abstracting the knobs in the "Interact" window into higher level concepts, such as transitions and color states, so that users do not need to remember which combination of knobs achieves certain effects. At the same time, participants appreciated having continuous control over the knobs for the immediate visual feedback. This suggests that a more effective interface could combine low level control with high level abstractions. In addition, our tool does not have error-handling methods for "invalid" SVG files that do not meet spacing conditions or closed-shape requirements, which can pose a challenge to novices. Thus, a possible direction for future work would be to devise methods for checking the feasibility of designs and handling them in the interface.

11.3 Materials and fabrication

While our fabrication process is an improvement over manual methods for constructing polarized light mosaics, it is not free of human error since users must remember to calibrate the strain direction of their cellophane sheets and place them into the laser cutter at the correct angle. One possible solution would be to add mechanisms for automatically correcting misalignments, such as a motorized turntable inside the laser cutter. As we did not evaluate our participants' fabrication-ability, a separate study that collects data on how users would fabricate a PLM would reveal more insights on the usability of our fabrication process.

12 CONCLUSION

In this paper, we presented the first software toolkit and digital fabrication process for PLMs with controlled color-changing behaviors. We introduced the design space that defines the color-changing effects and construction principles for Polagons. The application examples made by both the authors and external users showed how Polagons can be used for a range of domains, such as fashion, education, and visualization. Our technical evaluation demonstrated how Polagons can support hundreds of colors using only a few types of cellophane.

Creating digital fabrication processes for traditional making practices has the benefit of preserving art forms that are typically only accessible to skilled individuals. Austine Comarow, who was believed to have pioneered PLMs, unfortunately passed away in 2020 and was one of the few people in the world who could create intricate PLMs that animate in a controlled manner. We hope Polagons can expand the community of modern polarized light mosaicists and, by making the process accessible to makers, add a new programmable material to the diverse palette of options in HCI.

REFERENCES

[1] [n.d.]. *Color matching functions.*

[2] Lea Albaugh, James McCann, Lining Yao, and Scott E. Hudson. 2021. Enabling Personal Computational Handweaving with a Low-Cost Jacquard Loom. In *Proceedings of the 2021 CHI Conference on Human Factors in Computing Systems* (Yokohama, Japan) *(CHI '21)*. Association for Computing Machinery, New York, NY, USA, Article 497, 10 pages. https://doi.org/10.1145/3411764.3445750

[3] Ray Asahina, Takashi Nomoto, Takatoshi Yoshida, and Yoshihiro Watanabe. 2021. Realistic 3D Swept-Volume Display with Hidden-Surface Removal Using Physical Materials. In *2021 IEEE Virtual Reality and 3D User Interfaces (VR)*. 113–121. https://doi.org/10.1109/VR50410.2021.00032

[4] Bernd Bickel, Paolo Cignoni, Luigi Malomo, and Nico Pietroni. 2018. State of the Art on Stylized Fabrication. *Computer Graphics Forum* 37 (2018). http://vcg.isti.cnr.it/Publications/2018/BCMP18

[5] Susan Cousins Breen. 2021. *The Art of Polage*. https://www.swarthmore.edu/bulletin/archive/wp/july-2008_the-art-of-polage.html

[6] Eric Brockmeyer, Ivan Poupyrev, and Scott Hudson. 2013. PAPILLON: Designing Curved Display Surfaces with Printed Optics. In *Proceedings of the 26th Annual ACM Symposium on User Interface Software and Technology* (St. Andrews, Scotland, United Kingdom) *(UIST '13)*. Association for Computing Machinery, New York, NY, USA, 457–462. https://doi.org/10.1145/2501988.2502027

[7] Mayo Clinic. 2021. *U.S. coronavirus map: What do the trends mean for you?* https://www.mayoclinic.org/coronavirus-covid-19/map

[8] Austine Wood Comarow. 2021. *Austine Studios*. https://www.austine.com/

[9] Fernando Fuzinatto Dall'Agnol and Daniel Den Engelsen. 2012. Colors from polarizers and birefringent films. *Revista Brasileira de Ensino de Fisica* (2012). http://www.scielo.br/scielo.php?script=sci_arttext&pid=S1806-11172012000200005&nrm=iso

[10] SJ Edwards and AJ Langley. 1981. On producing colours using birefringence property of transparent, colourless stretched cellophane. *Leonardo* (1981), 187–190.

[11] Jonas Frich, Lindsay MacDonald Vermeulen, Christian Remy, Michael Mose Biskjaer, and Peter Dalsgaard. 2019. Mapping the landscape of creativity support tools in HCI. In *Proceedings of the 2019 CHI Conference on Human Factors in Computing Systems*. 1–18.

[12] Akash Garg, Andrew O Sageman-Furnas, Bailin Deng, Yonghao Yue, Eitan Grinspun, Mark Pauly, and Max Wardetzky. 2014. Wire mesh design. *ACM Transactions on Graphics* 33, 4 (2014).

[13] Arjan Gijsenij, Theo Gevers, and Joost Van De Weijer. 2011. Computational color constancy: Survey and experiments. *IEEE transactions on image processing* 20, 9 (2011), 2475–2489.

[14] MRSEC Education Group. 2021. *Creating Art with Polarized Light*. https://education.mrsec.wisc.edu/creating-art-polarized-light/

[15] Megan Hofmann, Lea Albaugh, Ticha Sethapakadi, Jessica Hodgins, Scott E Hudson, James McCann, and Jennifer Mankoff. 2019. KnitPicking textures: Programming and modifying complex knitted textures for machine and hand knitting. In *Proceedings of the 32nd annual ACM symposium on user interface software and technology*. 5–16.

[16] Melody Horn, Amy Traylor, and Leah Buechley. 2022. Slabforge: Design Software for Slab-Based Ceramics. In *CHI Conference on Human Factors in Computing Systems*. 1–12.

[17] Yuhua Jin, Isabel Qamar, Michael Wessely, Aradhana Adhikari, Katarina Bulovic, Parinya Punpongsanon, and Stefanie Mueller. 2019. Photo-Chromeleon: Re-Programmable Multi-Color Textures Using Photochromic Dyes. In *Proceedings of the 32nd Annual ACM Symposium on User Interface Software and Technology* (New Orleans, LA, USA) *(UIST '19)*. Association for Computing Machinery, New York, NY, USA, 701–712. https://doi.org/10.1145/3332165.3347905

[18] Hsin-Liu (Cindy) Kao, Manisha Mohan, Chris Schmandt, Joseph A. Paradiso, and Katia Vega. 2016. ChromoSkin: Towards Interactive Cosmetics Using Thermochromic Pigments. In *Proceedings of the 2016 CHI Conference Extended Abstracts on Human Factors in Computing Systems* (San Jose, California, USA) *(CHI EA '16)*. Association for Computing Machinery, New York, NY, USA, 3703–3706. https://doi.org/10.1145/2851581.2890270

[19] Yuki Katsumata, Wataru Yamada, and Hiroyuki Manabe. 2019. Optical See-Through Head-Mounted Display with Deep Depth of Field Using Pinhole Polarizing Plates. In *The Adjunct Publication of the 32nd Annual ACM Symposium on User Interface Software and Technology* (New Orleans, LA, USA) *(UIST '19)*. Association for Computing Machinery, 102–104.

[20] Rubaiat Habib Kazi, Kien Chuan Chua, Shengdong Zhao, Richard Davis, and Kok-Lim Low. 2011. SandCanvas: A Multi-Touch Art Medium Inspired by Sand Animation. In *Proceedings of the SIGCHI Conference on Human Factors in Computing Systems* (Vancouver, BC, Canada) *(CHI '11)*. Association for Computing Machinery, New York, NY, USA, 1283–1292. https://doi.org/10.1145/1978942.1979133

[21] Sawa Korogi, Takuya Kitade, and Wataru Yamada. 2020. Janus Screen: A Screen with Switchable Projection Surfaces Using Polarizers. In *Adjunct Publication of the 33rd Annual ACM Symposium on User Interface Software and Technology* (Virtual Event, USA) *(UIST '20 Adjunct)*. Association for Computing Machinery, New York, NY, USA, 123–125. https://doi.org/10.1145/3379350.3416144

[22] Mackenzie Leake, Gilbert Bernstein, Abe Davis, and Maneesh Agrawala. 2021. A mathematical foundation for foundation paper pieceable quilts. *ACM Trans. Graph.* 40, 4 (2021), 65–1.

[23] Rong-Hao Liang, Chao Shen, Yu-Chien Chan, Guan-Ting Chou, Liwei Chan, De-Nian Yang, Mike Y. Chen, and Bing-Yu Chen. 2015. *WonderLens: Optical Lenses and Mirrors for Tangible Interactions on Printed Paper*. Association for Computing Machinery, New York, NY, USA, 1281–1284. https://doi.org/10.1145/2702123.2702434

[24] Bruce Lindbloom. 2021. *XYZ to RGB: Bruce Lindbloom*. http://www.brucelindbloom.com/index.html?Eqn_XYZ_to_RGB.html

[25] Hao Liu, Xiao-Teng Zhang, Xiao-Ming Fu, Zhi-Chao Dong, and Ligang Liu. 2019. Computational Peeling Art Design. *ACM Trans. Graph.* 38, 4, Article 64 (July 2019), 12 pages. https://doi.org/10.1145/3306346.3323000

[26] Xuan Luo, Jason Lawrence, and Steven M. Seitz. 2017. Pepper's Cone: An Inexpensive Do-It-Yourself 3D Display. In *Proceedings of the 30th Annual ACM Symposium on User Interface Software and Technology* (Québec City, QC, Canada) *(UIST '17)*. Association for Computing Machinery, New York, NY, USA, 623–633. https://doi.org/10.1145/3126594.3126602

[27] James Mann. 2005. *Austine Wood Comarow: Paintings in Polarized Light*. Wasabi Publishing.

[28] James McCann, Lea Albaugh, Vidya Narayanan, April Grow, Wojciech Matusik, Jennifer Mankoff, and Jessica Hodgins. 2016. A compiler for 3D machine knitting. *ACM Transactions on Graphics (TOG)* 35, 4 (2016), 1–11.

[29] Leo Miyashita, Kota Ishihara, Yoshihiro Watanabe, and Masatoshi Ishikawa. 2016. ZoeMatrope: A System for Physical Material Design. *ACM Trans. Graph.* 35, 4, Article 66 (July 2016), 11 pages. https://doi.org/10.1145/2897824.2925925

[30] BA Morris. 2017. 4-Commonly Used Resins and Substrates in Flexible Packaging. *The Science and Technology of Flexible Packaging. Oxford: William Andrew Publishing* (2017), 69–119.

[31] Keith Muscutt. 1978. Projected Kinetic Displays and Photomicrographs Based on the Use of Polarized Light. *Leonardo* (1978). http://www.jstor.org/stable/1574003

[32] N.M. Neves, A.S. Pouzada, J.H.D. Voerman, and P.C. Powell. 1998. *Polymer engineering and science* 38, 10 (1998), 1770–1777. https://doi.org/10.1002/pen.10347

[33] Roshan Lalintha Peiris and Suranga Nanayakkara. 2014. PaperPixels: A Toolkit to Create Paper-Based Displays. In *Proceedings of the 26th Australian Computer-Human Interaction Conference on Designing Futures: The Future of Design* (Sydney, New South Wales, Australia) *(OzCHI '14)*. Association for Computing Machinery, New York, NY, USA, 498–504. https://doi.org/10.1145/2686612.2686691

[34] Roshan Lalintha Peiris, Mili John Tharakan, Adrian David Cheok, and Owen Noel Newton. 2011. AmbiKraf: A Ubiquitous Non-Emissive Color Changing Fabric Display. In *Proceedings of the 15th International Academic MindTrek Conference: Envisioning Future Media Environments* (Tampere, Finland) *(MindTrek '11)*. Association for Computing Machinery, New York, NY, USA, 320–322. https://doi.org/10.1145/2181037.2181096

[35] Thiadmer Riemersma. 2019. *Colour metric*. https://www.compuphase.com/cmetric.htm

[36] Alec Rivers, Andrew Adams, and Frédo Durand. 2012. Sculpting by numbers. *ACM Transactions on Graphics (TOG)* 31, 6 (2012), 1–7.

[37] Masato Sasaki, Takashi Nagamatsu, and Kentaro Takemura. 2019. Cross-Ratio Based Gaze Estimation for Multiple Displays Using a Polarization Camera. In *The Adjunct Publication of the 32nd Annual ACM Symposium on User Interface Software and Technology* (New Orleans, LA, USA) *(UIST '19)*. Association for Computing Machinery, New York, NY, USA, 1–3. https://doi.org/10.1145/3332167.3357095

[38] Toshiki Sato, Haruko Mamiya, Hideki Koike, and Kentaro Fukuchi. 2009. PhotoelasticTouch: Transparent Rubbery Tangible Interface Using an LCD and Photoelasticity. In *Proceedings of the 22nd Annual ACM Symposium on User Interface Software and Technology* (Victoria, BC, Canada) *(UIST '09)*. Association for Computing Machinery, New York, NY, USA, 43–50. https://doi.org/10.1145/1622176.1622185

[39] Nik Semenoff. 1984. Photographic Images and Optical Effects Using Birefringent Materials. *Leonardo* 17, 3 (1984), 180–184.

[40] Maria Shugrina, Jingwan Lu, and Stephen Diverdi. 2017. Playful Palette: An Interactive Parametric Color Mixer for Artists. *ACM Trans. Graph.* 36, 4, Article 61 (jul 2017), 10 pages. https://doi.org/10.1145/3072959.3073690

[41] Manlin Song, Chenyu Jia, and Katia Vega. 2018. Eunoia: Dynamically Control Thermochromic Displays for Animating Patterns on Fabrics *(UbiComp '18)*. Association for Computing Machinery, New York, NY, USA, 255–258. https://doi.org/10.1145/3267305.3267557

[42] Manlin Song and Katia Vega. 2018. HeartMe: Thermochromic Display as An Expression of Heart Health. In *Proceedings of the 2018 ACM Conference Companion Publication on Designing Interactive Systems* (Hong Kong, China) *(DIS '18 Companion)*. Association for Computing Machinery, New York, NY, USA, 311–314. https://doi.org/10.1145/3197391.3205393

[43] Zhao Tian, Charles J. Carver, Qijia Shao, Monika Roznere, Alberto Quattrini Li, and Xia Zhou. 2020. PolarTag: Invisible Data with Light Polarization. In *Proceedings of the 21st International Workshop on Mobile Computing Systems and Applications* (Austin, TX, USA) *(HotMobile '20)*. Association for Computing Machinery, New York, NY, USA, 74–79. https://doi.org/10.1145/3376897.3377854

[44] Cesar Torres, Jessica Chang, Advaita Patel, and Eric Paulos. 2019. Phosphenes: Crafting Resistive Heaters within Thermoreactive Composites. In *Proceedings*

of the 2019 on Designing Interactive Systems Conference (San Diego, CA, USA) *(DIS '19)*. Association for Computing Machinery, New York, NY, USA, 907–919. https://doi.org/10.1145/3322276.3322375
[45] Cesar Torres, Wilmot Li, and Eric Paulos. 2016. ProxyPrint: Supporting Crafting Practice through Physical Computational Proxies. In *Proceedings of the 2016 ACM Conference on Designing Interactive Systems (DIS '16)*. Association for Computing Machinery, New York, NY, USA, 158–169. https://doi.org/10.1145/2901790.2901828
[46] Cesar Torres, Jasper O'Leary, Molly Nicholas, and Eric Paulos. 2017. *Illumination Aesthetics: Light as a Creative Material within Computational Design.* Association for Computing Machinery, New York, NY, USA, 6111–6122. https://doi.org/10.1145/3025453.3025466
[47] Michael Wessely, Yuhua Jin, Cattalyya Nuengsigkapian, Aleksei Kashapov, Isabel P. S. Qamar, Dzmitry Tsetserukou, and Stefanie Mueller. 2021. ChromoUpdate: Fast Design Iteration of Photochromic Color Textures Using Grayscale Previews and Local Color Updates. In *Proceedings of the 2021 CHI Conference on Human Factors in Computing Systems* (Yokohama, Japan) *(CHI '21)*. Association for Computing Machinery, New York, NY, USA, Article 666, 13 pages. https://doi.org/10.1145/3411764.3445391
[48] Rundong Wu, Joy Xiaoji Zhang, Jonathan Leaf, Xinru Hua, Ante Qu, Claire Harvey, Emily Holtzman, Joy Ko, Brooks Hagan, Doug L James, et al. 2020. Weavecraft: an interactive design and simulation tool for 3D weaving. *ACM Trans. Graph.* 39, 6 (2020), 210–1.
[49] Wataru Yamada, Hiroyuki Manabe, Daizo Ikeda, and Jun Rekimoto. 2019. VARiable HMD: Optical See-Through HMD for AR and VR. In *The Adjunct Publication of the 32nd Annual ACM Symposium on User Interface Software and Technology* (New Orleans, LA, USA) *(UIST '19)*. Association for Computing Machinery, New York, NY, USA, 131–133. https://doi.org/10.1145/3332167.3356896
[50] Takatoshi Yoshida, Yoshihiro Watanabe, and Masatoshi Ishikawa. 2016. Phyxel: Realistic Display Using Physical Objects with High-Speed Spatially Pixelated Lighting. In *ACM SIGGRAPH 2016 Emerging Technologies* (Anaheim, California) *(SIGGRAPH '16)*. Association for Computing Machinery, New York, NY, USA, Article 18, 1 pages. https://doi.org/10.1145/2929464.2929476
[51] Jiani Zeng, Honghao Deng, Yunyi Zhu, Michael Wessely, Axel Kilian, and Stefanie. Mueller. 2021. Lenticular Objects: 3D Printed Objects with Lenticular Lens Surfaces that Can Change their Appearance Depending on the Viewpoint.. In *Proceedings of the 33th Annual ACM Symposium on User Interface Software and Technology (UIST '21)*. Association for Computing Machinery, New York, NY, USA, (to appear).

A MATERIAL EVALUATION

An important assumption of our color prediction algorithm is that the birefringence is constant for a given sheet of cellophane. To verify this, we created chips made from a single layer of 34mm×34mm cellophane. We cut 28 copies of each chip from different parts of the corresponding cellophane sheet, and after placing them between polarizers we photographed them under white light. For each cellophane type, we computed the average colors of each chip and calculated the standard deviation across the Red, Green, and Blue channels (Table 1). These statistics indicate that the colors in our 0.053mm cellophane samples have the highest variance relative to the other types, which suggests that our 0.053mm cellophane has the least consistent birefringence. While 0.053mm happens to the thickest and least birefringent cellophane type, there appears to be no correlation between thickness and variance or birefringence and variance. This can be attributed to random errors in the manufacturing process. Our tool helps to account for this by allowing users to estimate the birefringence of their sheets and record the estimations to the database (Section 5.4). This means if the user has a cellophane sheet with nonuniform birefringence, they can divide it into multiple parts and save each part as a separate cellophane type. Thus, users can improve the database by cataloguing their sheets in a more granular way.

Thickness (mm)	Birefringence (β)	Deviation (R,G,B)
0.023	0.01467	(3.90, 5.96, 7.60)
0.03	0.01668	(4.89, 4.36, 5.97)
0.035	0.01618	(3.77, 2.80, 8.96)
0.045	0.01518	(3.95, 7.46, 9.22)
0.053	0.01447	(11.05, 14.47, 22.01)

Table 1: Statistics for our supply of cellophane. Color deviation is on a scale of 0 to 255 (per channel).